Dysregulated Expression of the MicroRNA miR-137 and Its Target YBX1 Contribute to the Invasive Characteristics of Malignant Pleural Mesothelioma

Johnson, Thomas G; Schelch, Karin; Cheng, Yuen Y; Williams, Marissa; Sarun, Kadir H; Kirschner, Michaela B; Kao, Steven; Linton, Anthony; Klebe, Sonja; McCaughan, Brian C; Lin, Ruby C Y; Pirker, Christine; Berger, Walter; Lasham, Annette; van Zandwijk, Nico; Reid, Glen

Abstract: INTRODUCTION Malignant pleural mesothelioma (MPM) is an aggressive malignancy linked to asbestos exposure. On a genomic level, MPM is characterized by frequent chromosomal deletions of tumor suppressors, including microRNAs. MiR-137 plays a tumor suppressor role in other cancers, so the aim of this study was to characterize it and its target Y-box binding protein 1 (YBX1) in MPM. METHODS Expression, methylation, and copy number status of miR-137 and its host gene MIR137HG were assessed by polymerase chain reaction. Luciferase reporter assays confirmed a direct interaction between miR-137 and Y-box binding protein 1 gene (YBX1). Cells were transfected with a miR-137 inhibitor, miR-137 mimic, and/or YBX1 small interfering RNA, and growth, colony formation, migration and invasion assays were conducted. RESULTS MiR-137 expression varied among MPM cell lines and tissue specimens, which was associated with copy number variation and promoter hypermethylation. High miR-137 expression was linked to poor patient survival. The miR-137 inhibitor did not affect target levels or growth, but interestingly, it increased miR-137 levels by means of mimic transfection suppressed growth, migration, and invasion, which was linked to direct YBX1 downregulation. YBX1 was overexpressed in MPM cell lines and inversely correlated with miR-137. RNA interference-mediated YBX1 knockdown significantly reduced cell growth, migration, and invasion. CONCLUSIONS MiR-137 can exhibit a tumor-suppressive function in MPM by targeting YBX1. YBX1 knockdown significantly reduces tumor growth, migration, and invasion of MPM cells. Therefore, YBX1 represents a potential target for novel MPM treatment strategies.

DOI: https://doi.org/10.1016/j.jtho.2017.10.016

Johnson, Thomas G; Schelch, Karin; Cheng, Yuen Y; Williams, Marissa; Sarun, Kadir H; Kirschner, Michaela B; Kao, Steven; Linton, Anthony; Klebe, Sonja; McCaughan, Brian C; Lin, Ruby C Y; Pirker, Christine; Berger, Walter; Lasham, Annette; van Zandwijk, Nico; Reid, Glen (2018). Dysregulated Expression of the MicroRNA miR-137 and Its Target YBX1 Contribute to the Invasive Characteristics of Malignant Pleural Mesothelioma. Journal of Thoracic Oncology, 13(2):258-272.
DOI: https://doi.org/10.1016/j.jtho.2017.10.016

ORIGINAL ARTICLE

Dysregulated Expression of the MicroRNA miR-137 and Its Target YBX1 Contribute to the Invasive Characteristics of Malignant Pleural Mesothelioma

Thomas G. Johnson, BSc,[a] Karin Schelch, PhD,[a] Yuen Y. Cheng, PhD,[a,b] Marissa Williams, BSc,[a,b] Kadir H. Sarun, BSc,[a] Michaela B. Kirschner, PhD,[c] Steven Kao, PhD,[a,b,d] Anthony Linton, PhD,[a,b,e] Sonja Klebe, PhD,[f,g] Brian C. McCaughan, FRACS,[g,h] Ruby C. Y. Lin, PhD,[a,i] Christine Pirker, PhD,[j] Walter Berger, PhD,[j] Annette Lasham, PhD,[k] Nico van Zandwijk, PhD,[a,b] Glen Reid, PhD[a,b,*]

[a]*Asbestos Diseases Research Institute, Sydney, Australia*
[b]*School of Medicine, University of Sydney, Sydney, Australia*
[c]*Division of Thoracic Surgery, University Hospital Zurich, Zurich, Switzerland*
[d]*Department of Medical Oncology, Chris O'Brien Lifehouse, Sydney, Australia*
[e]*Concord Cancer Centre, Concord Repatriation General Hospital, Sydney, Australia*
[f]*Department of Anatomical Pathology, Flinders University*
[g]*Department of Anatomical Pathology, SA Pathology at Flinders Medical Centre, Adelaide, Australia*
[h]*Sydney Cardiothoracic Surgeons, RPAH Medical Centre, Sydney, Australia*
[i]*School of Medical Sciences, University of New South Wales, Sydney, Australia*
[j]*Institute of Cancer Research, Department of Medicine I, Medical University of Vienna, Vienna, Austria*
[k]*Department of Molecular Medicine and Pathology, School of Medical Sciences, University of Auckland, Auckland, New Zealand*

Received 22 June 2017; revised 10 October 2017; accepted 21 October 2017
Available online - 4 November 2017

ABSTRACT

Introduction: Malignant pleural mesothelioma (MPM) is an aggressive malignancy linked to asbestos exposure. On a genomic level, MPM is characterized by frequent chromosomal deletions of tumor suppressors, including microRNAs. MiR-137 plays a tumor suppressor role in other cancers, so the aim of this study was to characterize it and its target Y-box binding protein 1 (YBX1) in MPM.

Methods: Expression, methylation, and copy number status of miR-137 and its host gene *MIR137HG* were assessed by polymerase chain reaction. Luciferase reporter assays confirmed a direct interaction between miR-137 and Y-box binding protein 1 gene (*YBX1*). Cells were transfected with a miR-137 inhibitor, miR-137 mimic, and/or *YBX1* small interfering RNA, and growth, colony formation, migration and invasion assays were conducted.

Results: MiR-137 expression varied among MPM cell lines and tissue specimens, which was associated with copy number variation and promoter hypermethylation. High miR-137 expression was linked to poor patient survival. The miR-137 inhibitor did not affect target levels or growth, but interestingly, it increased miR-137 levels by means of mimic transfection suppressed growth, migration, and invasion, which was linked to direct YBX1 downregulation. YBX1 was overexpressed in MPM cell lines and inversely correlated with miR-137. RNA interference–mediated YBX1 knockdown significantly reduced cell growth, migration, and invasion.

Conclusions: MiR-137 can exhibit a tumor-suppressive function in MPM by targeting YBX1. YBX1 knockdown significantly reduces tumor growth, migration, and invasion of MPM cells. Therefore, YBX1 represents a potential target for novel MPM treatment strategies.

***Corresponding author.**

Mr. Johnson and Dr. Schelch contributed equally to this work.

Disclosure: Dr. Kao reports personal fees from Pfizer, MSD, Bristol-Myers Squibb, AstraZeneca, and Roche outside the submitted work. Dr. Linton reports nonfinancial support from AstraZeneca and Bristol-Myers Squibb, outside the submitted work. Dr. Reid has a patent, US 9,006,200, issued. The remaining authors declare no conflict of interest.

Address for correspondence: Glen Reid, PhD, Asbestos Diseases Research Institute, PO Box 3628, Rhodes NSW 2138, Sydney, Australia. E-mail: glen.reid@sydney.edu.au

ISSN: 1556-0864

https://doi.org/10.1016/j.jtho.2017.10.016

Keywords: Malignant pleural mesothelioma; Y-box binding protein-1; YBX1; miR-137; microRNA; Cancer

Introduction

Malignant pleural mesothelioma (MPM) is an aggressive malignancy arising from the mesothelial lining of the pleural cavity after asbestos exposure. Present therapeutic options for MPM are limited—the current standard combination of cisplatin and pemetrexed is largely palliative and provides a modest median survival of 12.1 months.[1,2] Despite resounding epidemiological evidence associating asbestos consumption and MPM incidence, nine of the 10 most populous countries in the world have yet to implement a complete asbestos ban.[3,4] Factoring in the extended latency period between asbestos exposure and MPM development (30–50 years), global MPM incidence is expected to rise within the next decade.[3] Therefore, better characterization of MPM biology to aid in the development of new therapeutic strategies is essential.

Next-generation sequencing data has confirmed an association between MPM development and the loss of three key tumor suppressors.[5] Downregulation of p16 (encoded by cyclin-dependent kinase inhibitor 2A gene [*CDKN2A*]) is linked to copy number loss of region 9p21-22.[6] p16 acts on cyclin-dependent kinases such as cyclin-dependent kinase 4, and homozygous deletion of *CDKN2A* has been reported in 65% to 70% of MPM samples.[6,7] The deubiquitinating hydrolase BRCA1 associated protein 1 (BAP1) functions in DNA damage response and cell cycle regulation,[8] and the BRCA1 associated protein 1 gene (*BAP1* gene) located on chromosome 3p21.1 is deleted in 40% of MPM cases.[9] Finally, merlin, a cytoskeletal protein encoded by neurofibromin 2 gene (*NF2*) at 22q12.2, mediates contact inhibition in normal cells and is an upstream suppressor of the Hippo pathway.[10] It is deleted in more than 40% MPM cases, with dysregulation of the Hippo pathway occurring in 80%.[11]

In addition to these regions, deletion of 1p21-22 has been reported in up to 70% of MPM cases,[9,12] but to our knowledge there is little information regarding the implications of 1p21-22 deletion for MPM biology. Interestingly, the deletion of this region was significantly associated with 9p21-22 locus loss in MPM,[13] which (in addition to *CDKN2A*) is also home to the microRNA (miRNA) miR-31, a tumor suppressor that is also frequently lost through homozygous deletion of this region.[14] miRNAs are small, noncoding RNAs that are fundamentally involved in the regulation of almost all biological processes.[15] Many are located at fragile sites and are often silenced in cancer through deletion or promoter hypermethylation.[15,16] The dysregulation of numerous miRNAs has been linked to the development and progression of human cancer, and recently, miRNA-based therapeutics have shown promise in tumors such as MPM.[17,18]

As the consequences of 1p21-22 locus deletion in MPM biology are poorly understood, we investigated the role of miR-137 in MPM because its host gene is located at 1p21.3. MiR-137 has demonstrated tumor-suppressive activity in colorectal cancer (CRC) and glioblastoma multiforme,[19,20] although its role in MPM is unknown. Here, we characterize the expression and functions of miR-137 in MPM and explore the role of one of its targets, Y-box binding protein-1 (YBX1), in the context of MPM biology.

Materials and Methods

Cell Culture

Cells were maintained in Roswell Park Memorial Institute medium supplemented with 10% heat-inactivated fetal bovine serum (both Thermo Fisher Scientific, Waltham, MA) in a humidified atmosphere (5% CO_2 at 37 °C). The cell lines and their source and histological subtype are listed in Supplementary Table 1. Cells were routinely monitored for mycoplasma, and their identity was confirmed by short tandem repeat profiling (Australian Genome Research Facility).

Patient Samples

We obtained formalin-fixed, paraffin-embedded (FFPE) tissue samples from two cohorts (n = 115) of patients who underwent extrapleural pneumonectomy from 1994 to 2009 at Royal Prince Alfred and Strathfield Private Hospitals, Sydney, Australia, or pleurectomy and/or decortication (P/D) between 1991 and 2009 at Royal Prince Alfred Hospital.[21,22] FFPE pleural and pericardium control samples (n = 23) were obtained through nonmalignant cardiovascular surgery. A third series, consisting of fresh frozen (F/F) samples (n = 12), was obtained from patients who underwent extrapleural pneumonectomy, pleurectomy and/or decortication, or video-assisted thoracoscopic surgery from 2009 to 2012 at Royal Prince Alfred and Strathfield Private Hospitals, Sydney, Australia. The use of all samples was approved by the Human Research Ethics Committee at Concord Repatriation General Hospital, Sydney, Australia.

Transfection with MicroRNA Inhibitors, Mimics, and siRNAs

miRCURY miR-137 locked nucleic acid (LNA) inhibitor and miRCURY LNA inhibitor negative controls were purchased from Exiqon (Vedbæk, Denmark) (Supplementary Table 2). MiR-137 mimic, Y-box binding protein 1 gene (*YBX1*)-specific small interfering RNA (siRNA), and validated negative control mimic and siRNA were purchased from Shanghai GenePharma (Shanghai, China) (see Supplementary Table 2). Cells were reverse-transfected

using 0.1% Lipofectamine RNAiMAX (Thermo Fisher Scientific) as per the manufacturer's protocol.

Copy Number Variation

Genomic DNA was extracted using the QIAamp DNA mini kit (Qiagen, Hilden, Germany). Primer sequences and a schematic representation of their location are in Supplementary Table 3 and Supplementary Fig. 1. Copy number variation (CNV) of the miR-137 host gene (*MIR137HG*) region was assessed by droplet digital polymerase chain reaction (PCR) using Evagreen (Bio-Rad, Hercules, CA). Ribonuclease P/MRP subunit 30 gene (*RPP30*) was used as a reference gene and *Hind*III was used to digest DNA (New England Biolabs, Ipswich, MA). Droplets were generated with a QX200 droplet generator and read on a QX200 droplet reader (both Bio-Rad) per the manufacturer's guidelines.

MSP and Genomic DNA Extraction

Methylated- and unmethylated-specific primers (Supplementary Table 4) were designed within CpG islands surrounding the *MIR137HG* gene by using the MethPrimer methylation mapping program,[23] as per standard methylation-specific polymerase chain reaction (MSP) design guidelines. Genomic DNA was extracted. Buffy coat DNA and EpiTech Control unmethylated DNA (Qiagen) served as methylation negative controls. HCT116 DNA served as a methylation positive control, as *MIR137HG* is methylated in this cell line.[19] Bisulphite conversion was conducted with an EZ DNA methylation kit (Zymo Research, Irvine, CA). End point PCR (AmpliTaq GOLD DNA kit, Thermo Fisher Scientific) and quantitative MSP (qMSP) using HCT116 as a methylation calibrator was conducted with the aforementioned primers and the KAPA SYBR FAST kit (KAPA Biosystems, Wilmington, MA) per the manufacturer's guidelines (see Supplementary Table 4). Methylation-specific primers for a region of the actin beta gene (*ACTB*) which no CpG sites were found were used as a reference gene for qMSP (see Supplementary Table 4). End point PCR products were run on an agarose gel and visualized on a Kodak Gel Logic 2200 imaging system (Eastman Kodak Company, Rochester, NY).

Assessing pri-miR-137 Expression in Mouse MPM Xenograft Models

Xenografts were grown by injecting H226 and MSTO cells subcutaneously into BALB/c nude mice. The mice were killed and the tumors were surgically removed. Samples were snap-frozen and homogenized, and RNA was isolated by using TRIzol. The use of animals was approved by the Sydney South West Area Health Service (2011-007). The primers and probes for human or mouse pri-miR-137 are in Supplementary Table 5.

Luciferase Reporter Assay

A fragment of *YBX1* 3′ untranslated region containing the miR-137 binding site was cloned from cDNA from SPC212 cells and amplified using AmpliTaq Gold 360 (Promega, Madison, WI) with specific primers (Supplementary Table 6). PCR amplicons were cloned into the TOPO TA vector (Thermo Fisher Scientific) and subcloned into the pSiCheck2 plasmid (Promega). The sequence was confirmed by Sanger sequencing at the Ramaciotti Centre (University of New South Wales, Sydney, Australia). The reporter construct (1 μg), with miRNA mimic or controls (5 nM) were transfected in 2×10^5 cells in six-well plates. A dual luciferase assay (Promega) was performed per the manufacturer's protocol 48 hours after transfection.

Protein Isolation and Western Blot

Cells were transfected with 5 nM miRNA mimic, siRNAs, or controls. After indicated time points, protein was isolated in radioimmunoprecipitation assay buffer (including protease inhibitor cocktail [Roche Diagnostics, Mannheim, Germany]) and the concentration was measured by using a Pierce bicinchoninic protein assay (Thermo Fisher Scientific). Proteins were separated by sodium dodecyl sulfate polyacrylamide gel electrophoresis and blotted onto polyvinylidene fluoride membranes. Immunodetection was performed using a monoclonal rabbit anti–YBX1 antibody (Abcam, Cambridge, UK; 1:1000). β-actin (Sigma Aldrich, Dorset, UK) served as a loading control. Densitometry was performed with ImageJ.[24]

Videomicroscopy

Cells (2×10^3) were seeded into eight-well chamber slides (Ibidi, Planegg, Germany). Forty-eight hours after transfection with 5 nM of either miR-137 mimic, *YBX1* siRNA, or controls, cells were treated with 2 μg/mL mitomycin-C for 2 hours. The next day, cells were stained with cell tracker (Abcam) for 30 minutes. Videos were generated using a PALM MicroBeam laser microdissection microscope (Zeiss, Oberkochen, Germany) with pictures taken every 30 minutes for 25 hours. The distance migrated by at least 40 single cells was manually tracked with ImageJ software.

Agarose-Spot Invasion Assay

Cells (1.2×10^5) were transfected with 5 nM miR-137 mimic, *YBX1* siRNA, or the respective controls. The next day, cells were treated with 2 μg/mL mitomycin-C for 2 hours and then replated into 24-well plates prepared with agarose spots consisting of 7.5 μL 2% low-melting agar containing 0.4% fetal bovine serum (adapted from Cheng et al. 2014[25]). Images were taken after 48 hours and quantified with ImageJ software.

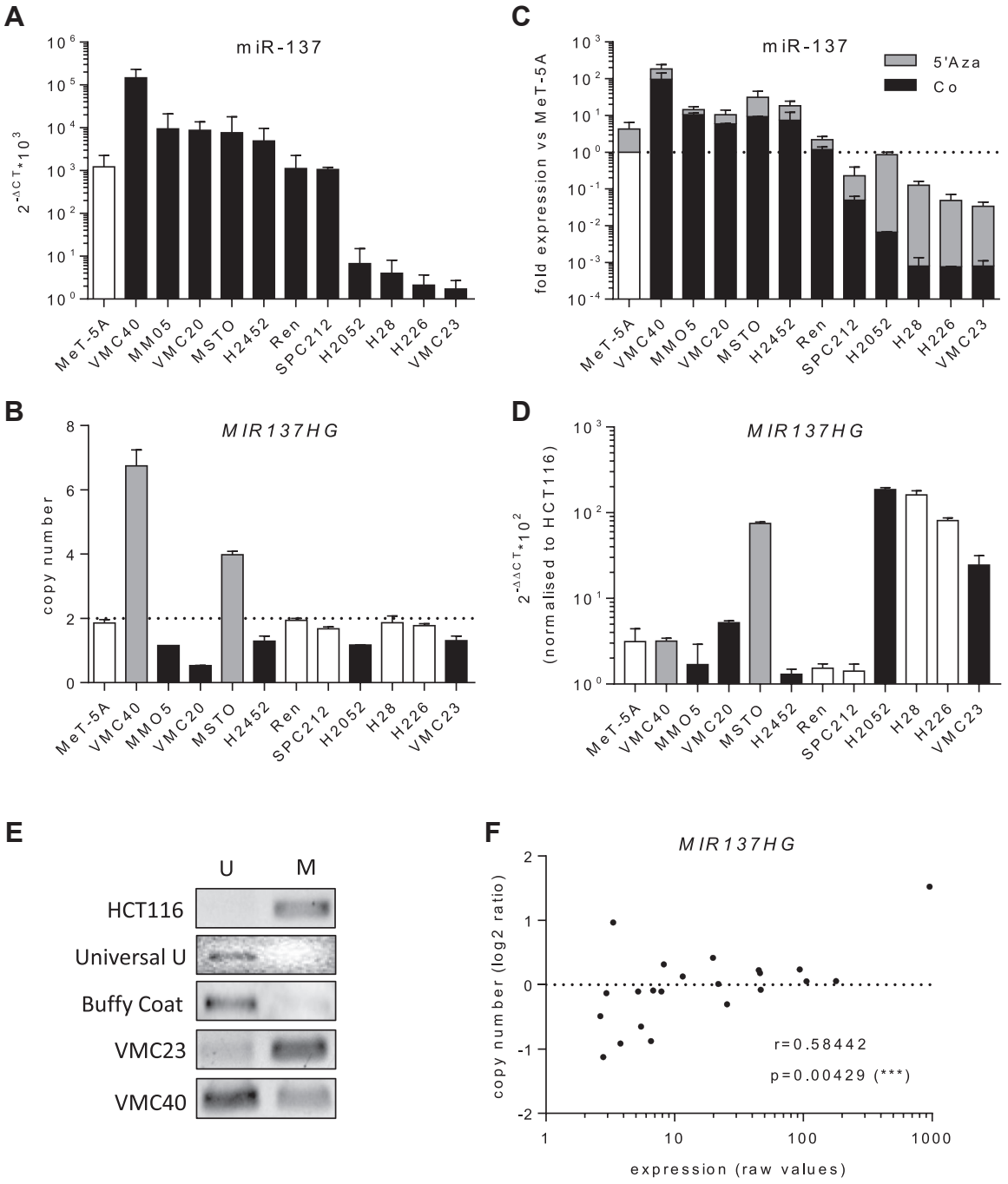

Figure 1. miR-137 is variably expressed in malignant pleural mesothelioma (MPM) cell lines because of copy number variation and promoter hypermethylation. (*A*) Endogenous expression of miR-137 in cell lines compared with RNA U6, small nuclear 6, pseudogene, determined by reverse-transcriptase quantitative polymerase chain reaction (PCR). MeT-5A (*white*) served as the control (Co), MPM cell lines are in black (*B*) Copy number (*white*, no change; *black*, loss, and *gray*, gain) of MIR137 host gene (*MIR137HG*) in cell lines normalized to the ribonuclease P protein subunit p30 (*RPP30*) assessed by digital droplet PCR. (*C*) Expression of miR-137 was determined by reverse-transcriptase PCR after treatment with either 5 μM 5-azacitidine (5-Aza [*gray*]) or vehicle (Co [*black*]). (*D*) Quantitative methylation-specific PCR of the *MIR137HG* of cell lines using the actin beta gene (*ACTB*) as a reference gene and HCT116 as the methylation calibrator. (*E*) Methylation-specific PCR products run on a 1.5% (wt/vol) agarose gel. (F) The relationship (significant using Spearman's rank correlation, $r = 0.58442$, $p = 0.00429$) between miR-137 expression and *MIR137HG* copy number status in MPM cell lines (n = 22), as determined by expression array and array comparative genomic hybridization, respectively. ***$p < 0.001$. U, unmethylated primer pair; M, methylated primer pair.

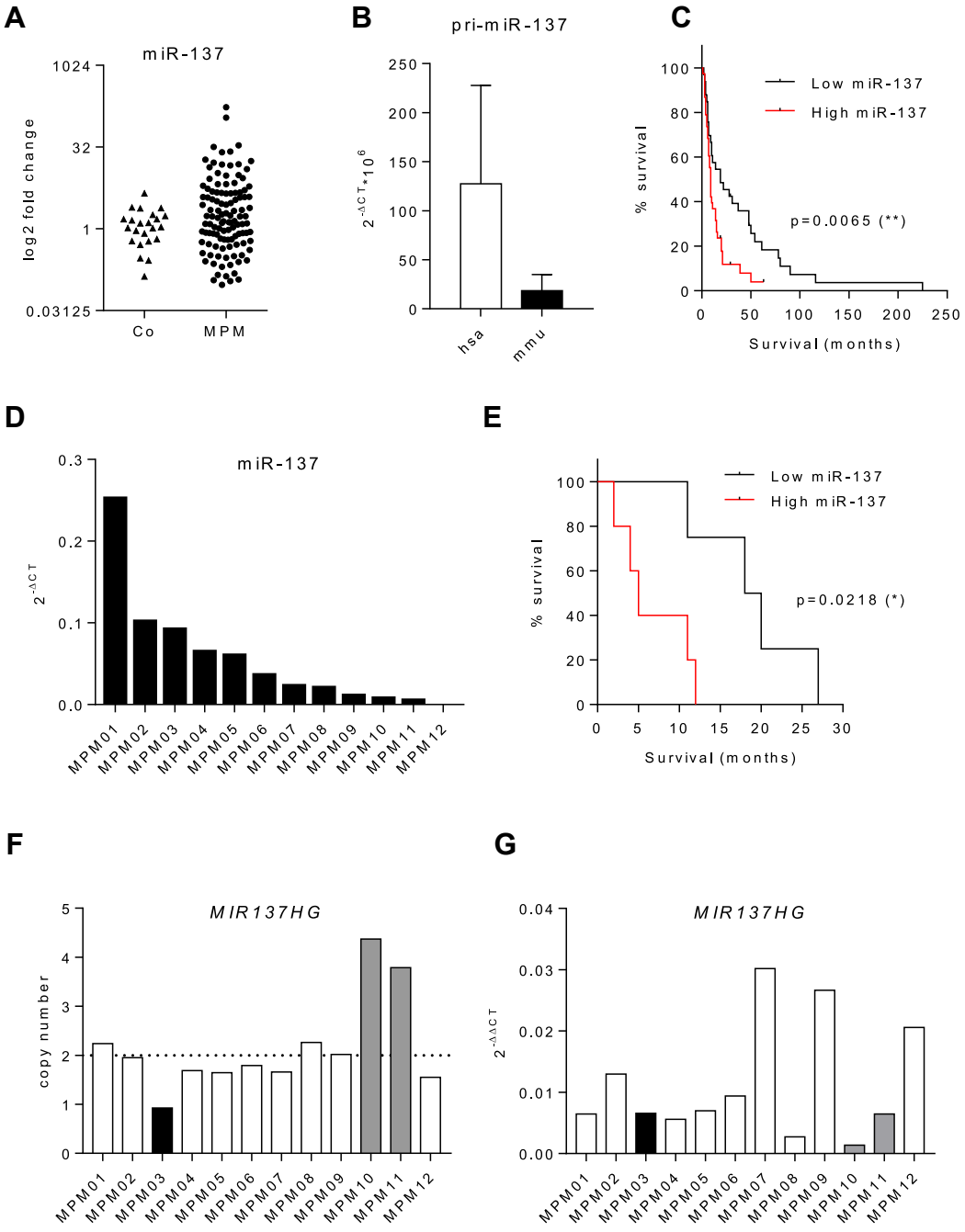

Figure 2. Differential expression of miR-137 because of promoter methylation has prognostic significance in patients with malignant pleural mesothelioma (MPM). (*A*) Levels of miR-137 in MPM (n = 115) and mesothelial (control [Co]) (n = 23) formalin-fixed paraffin-embedded tissue specimens determined by reverse-transcriptase quantitative polymerase chain reaction (RT-qPCR) using RNA U6, small nuclear 6, pseudogene gene (*RNU6B*) as a reference gene. Data are expressed as fold change relative to the mean of healthy Co samples (log2(ΔΔCq)) plus or minus the SE of the mean. (*B*) Kaplan-Meier curve showing prognostic significance of miR-137 in the cohort of formalin-fixed paraffin-embedded samples (significant using the Mantle-Cox test [$p = 0.0065$]). High- and low-expressing groups were dichotomized by a more than twofold change to the median of the cohort. (*C*) Expression of hsa- and mmu-pri-miR-137 in mouse xenografts with human MPM cells, determined by RT-qPCR using 18S as a reference gene and expressed as $2^{-dCT} \times 10^6$. (*D*) Expression of miR-137 in the cohort of fresh frozen (F/F) samples, determined by RT-qPCR using *RNU6B* as a reference gene. (*E*) Kaplan-Meier survival curve of the cohort of F/F samples (significant using the Mantle-Cox test [$p = 0.0218$]). (*F*) Copy number variation of the cohort of F/F samples (*white*, no change; *black*, loss; and *gray*, gain) of MIR137 host gene (*MIR137HG*) in cell lines normalized to the ribonuclease P protein subunit p30 (*RPP30*) assessed by digital droplet polymerase chain reaction. (*G*) Quantitative methylation-specific polymerase chain reaction of *MIR137HG* of the cohort of F/F patient samples using the actin beta gene (*ACTB*) as a reference gene and HCT116 as the methylation calibrator. *$p < 0.05$, **$p < 0.01$.

Statistical Analysis

Unless stated otherwise, data are presented as mean plus or minus SE of the mean. Statistical analysis was carried out with Prism7.0 software (GraphPad Software, La Jolla, CA), Social Science Statistics online calculators (Kirkman, TW. Statistics to use. http://www.physics.csbsju.edu/stats; date accessed: August 24, 2017), and SPSS software (IBM Corp., Armonk, NY). A Kolmogorov-Smirnov test was used to determine whether data were normally distributed. A two-tailed unpaired *t* test was used to test for significant differences for normally distributed data. A two-tailed Mann-Whitney test with a significance level of 0.05 was conducted to test for significant differences on data that were not normally distributed. A one-way analysis of variance was conducted to analyze the proliferation assay data. Pearson correlation was used to investigate correlations of normally distributed data. Spearman's rank correlation was used to investigate correlations of data that were not normally distributed. Patient survival was tested by using a Mantel-Cox Kaplan Meier test. All *p* values less than 0.05 were considered statistically significant.

Details on additional methods including RNA isolation, quantitative PCR (qPCR), gene expression arrays, and standard growth and migration assays are described in the Supplementary Materials and Methods.

Results

Copy Number Variation and Promoter Hypermethylation Contribute to Aberrant miR-137 Expression in MPM

Basal miR-137 expression was determined in a panel of 11 MPM cell lines and the immortalized mesothelial cell line MeT-5A by RT-qPCR. MiR-137 was aberrantly expressed in most cell lines compared with MeT-5A. Four cell lines (H2052, H28, H226, and VMC23) expressed notably lower and one (VMC40) expressed notably higher miR-137 levels (Fig. 1*A*). To better understand this variable expression, we determined the copy number status of the exon encoding *MIR137HG* by digital droplet PCR. CNV was evident in seven of 11 cell lines (Fig. 1*B*). Although there was no significant correlation, two low-expressing cell lines (H2052 and VMC23) also exhibited loss of heterozygosity (LOH), and VMC40 and MSTO, which had among the highest levels of miR-137, displayed copy number gains.

We suspected that methylation of the *MIR137HG* promoter also contributes to the variable expression observed, so we investigated the effects of the demethylating agent 5-aza-cytidine (5-Aza) on miR-137 expression. 5-Aza upregulated miR-137 in all cell lines, particularly in the low-expressing subgroup, which demonstrated marked miR-137 reexpression (Fig. 1*C*). To confirm that the response to 5-Aza was due to methylation of the *MIR137HG* promoter, we conducted qMSP. The four low-expressing cell lines exhibited high miR-137 promoter methylation, whereas high-expressing cell lines exhibited low promoter methylation; the exception was MSTO, which also displays gene amplification (Fig. 1*D*). We then conducted end point MSP to confirm our qMSP data in the highest- (VMC40) and lowest- (VMC23) expressing cell lines (Fig. 1*E*).

To validate our CNV data, we performed gene expression arrays and array comparative genomic hybridization to assess *MIR137HG* expression and copy number status in a larger, partially overlapping set of cell lines (n = 22). In that panel, a similar variable expression pattern was seen (Supplementary Fig. 2), and there was significant correlation between miR-137 expression and *MIR137HG* copy number status (Spearman's $r = 0.58442$, $p = 0.00429$) (Fig. 1*F*).

To see whether the variable miR-137 expression was also evident in MPM tumor samples, we determined the expression of miR-137 in 115 MPM tumor and 23 normal mesothelial FFPE tissue specimens. Consistent with our results in cell lines, both MPM tumor and normal mesothelial tissue exhibit highly variable miR-137 expression (Fig. 2*A*). To assess the potential contribution of stromal cells to miR-137 levels, we measured human and mouse pri-miR-137 expression in mouse xenografts. We found that hsa-pri-miR-137 expression was overwhelmingly higher than mmu-pri-miR-137 expression, suggesting that the observed miR-137 primarily originates from tumor cells and stromal contribution is limited (Fig. 2*B*). The effect of high and low miR-137 levels (defined by more than a twofold change to the median of the tumor cohort) on patient survival was analyzed by utilizing a Kaplan-Meier curve (Fig. 2*C*). Patients with low miR-137 expression survived significantly longer than patients with high miR-137 expression ($p = 0.0065$, Mantle-Cox test). To validate these findings and to analyze CNV and methylation in patient samples, we determined the expression of miR-137 in a smaller cohort of F/F samples (n = 12). We found a similar spread of expression (Fig. 2*D*) and, when analyzed with the same parameters as the FFPE cohort, patients with low miR-137 expression also survived significantly

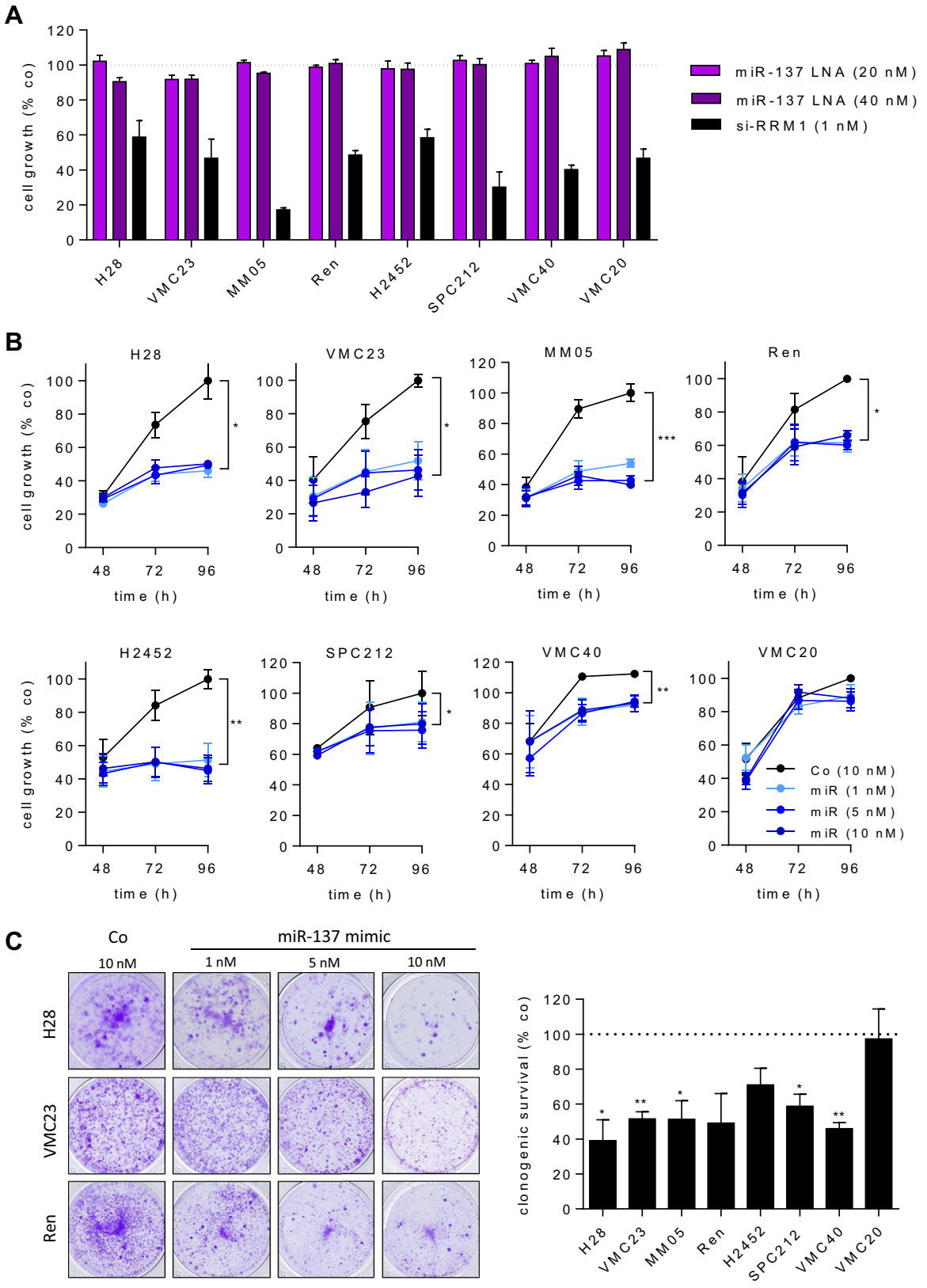

Figure 3. miR-137 mimic inhibits the proliferation and colony formation ability of malignant pleural mesothelioma (MPM) cell lines. (*A*) Growth inhibition assay of MPM cell lines 96 hours after transfection with miR-137 locked nucleic acid (at 20 nM and 40 nM) as well as RRM1 siRNA (1 nM) normalized to two locked nucleic acid controls (Cos) (40 nM). Data are expressed as the mean plus or minus SE of the mean of three independent experiments performed in triplicate. (*B*) Growth of MPM cell lines was followed for 96 hours after transfection of miR-137 or Co mimic at the indicated concentrations. Data are expressed as

longer than those with high expression ($p = 0.0218$) (Fig. 2*E*). MiR-137 was not associated with age, sex, or histological subtype in either the cohort of FFPE samples or the cohort of F/F samples. Clinicopathological patient characteristics are summarized in Supplementary Tables 7 and 8. CNV of the *MIR137HG* was determined by using the same protocol as in Figure 1*B*, and although one sample demonstrated LOH and two copy number gains, this did not correlate with expression (Fig. 2*F*). We conducted qMSP using the same protocol as in Figure 1*D*. Of the six samples displaying relatively low miR-137 expression, three displayed higher levels of methylation, which was consistent with our cell line data (Fig. 2*G*).

miR-137 Suppresses MPM Cell Growth and Colony Formation

As we showed that high miR-137 expression is associated with poor patient outcome, we investigated the effect on growth of inhibiting its expression with a miR-137 miRCURY LNA inhibitor in eight MPM cell lines. Inhibitor transfection resulted in a decrease of miR-137 expression (Supplementary Fig. 3), but no significant effect on growth was observed in any cell line over 96 hours (Fig. 3*A*). As a subgroup of MPM cells lines and patient samples displayed reduced expression of miR-137, we also investigated the effect of increasing miR-137 levels using a miRNA mimic. Mimic transfection led to increased miR-137 levels (see Supplementary Fig. 3) as well as significant growth inhibition over 96 hours in seven of eight cell lines (Fig. 3*B*). Generally, cell lines expressing low or moderate endogenous miR-137 (MM05, Ren, H2452, SPC212) displayed greater growth inhibition in response to miR-137 mimic, compared with the higher-expressing cell lines (VMC40, VMC20). MiR-137 mimic transfection also disrupted colony formation in five of eight MPM cell lines (Fig. 3*C*).

miR-137 Regulates Cell Migration and Invasion

The effect of miR-137 on cell migration was assessed by live cell videomicroscopy and manual single-cell tracking. MiR-137 mimic transfection significantly reduced the motility of low (H28, VMC23) or moderate (SPC212) miR-137–expressing cells compared with mimic control transfection. VMC40, which expresses high miR-137 levels, was unaffected (Fig. 4*A* and *B*). Wound healing assays performed on the same cell lines after transfection with miR-137 or control mimic confirmed these observations (Fig. 4*C*). Invasion was investigated by using agarose-spot assays after mimic transfection, which significantly reduced the invasive potential of all MPM cells. Again, these effects were more prominent in cell lines expressing low-to-moderate levels of miR-137 (SPC212, H28, and VMC23) (Fig. 4*D*).

miR-137 Targets the Oncoprotein YBX1, Which Is Highly Expressed in MPM

After transfecting six MPM cell lines with miR-137 mimic and miR-137 LNA inhibitor, we quantified the expression of several cancer-associated miR-137 target genes. AKT/serine threonine kinase 2 gene (*AKT2*), cyclin-dependent kinase 6 gene (*CDK6*), and *YBX1* transcripts were unaffected by miR-137 LNA inhibitor transfection but were significantly down-regulated in response to miR-137 mimics (Fig. 5*A*). We then focused on the miR-137/*YBX1* interaction, as it was the most prominently down-regulated target. MiR-137 also down-regulated YBX1 protein in three of four cell lines; VMC40 (with high miR-137) showed no change in YBX1 levels, although it has low basal YBX1 expression (Fig. 5*B*). The 3′ untranslated region of *YBX1* linked to a luciferase reporter demonstrated that miR-137 directly binds to *YBX1* (Fig. 5*C*).

Basal YBX1 protein and *YBX1* mRNA levels were analyzed by Western blot and RT-qPCR in all MPM cell lines and the mesothelial cell line MeT-5A and were found to be significantly correlated (Pearson's $r = 0.6584$, $p = 0.0276$, Supplementary Fig. 4). YBX1 protein expression showed a significant inverse correlation with basal miR-137 expression (Spearman's $r = -0.64693$, $p = 0.03145$) (Fig. 5*D*). Importantly, irrespective of basal miR-137 expression, YBX1 levels were consistently higher in MPM cell lines than in the MeT-5A cell line (see Fig. 5*D* [*red line*]), implying an important role of YBX1 in MPM biology.

YBX1 Knockdown Decreases MPM Cell Proliferation, Colony Formation, Migration, and Invasion

To determine whether downregulation of YBX1 contributes to the tumor-suppressing activity of miR-137, we performed several assays after transfection with YBX1–specific siRNA alone and in combination with miR-137 mimic. RNA interference–mediated YBX1 knockdown significantly decreased *YBX1* mRNA and YBX1 protein levels (Supplementary Fig. 5). Proliferation

the mean plus or minus SE of the mean of the percentage of Co-transfected cells at 96 hours and is representative of three independent experiments performed in triplicate. (*C*) Representative pictures of the colonies formed after transfection with miR-137 or Co mimic transfection. The histogram shows quantification of crystal violet in colonies formed by cells transfected with miR-137 (5 nM) normalized to Cos. $^{*}p < 0.05$, $^{**}p < 0.01$, $^{***}p < 0.001$.

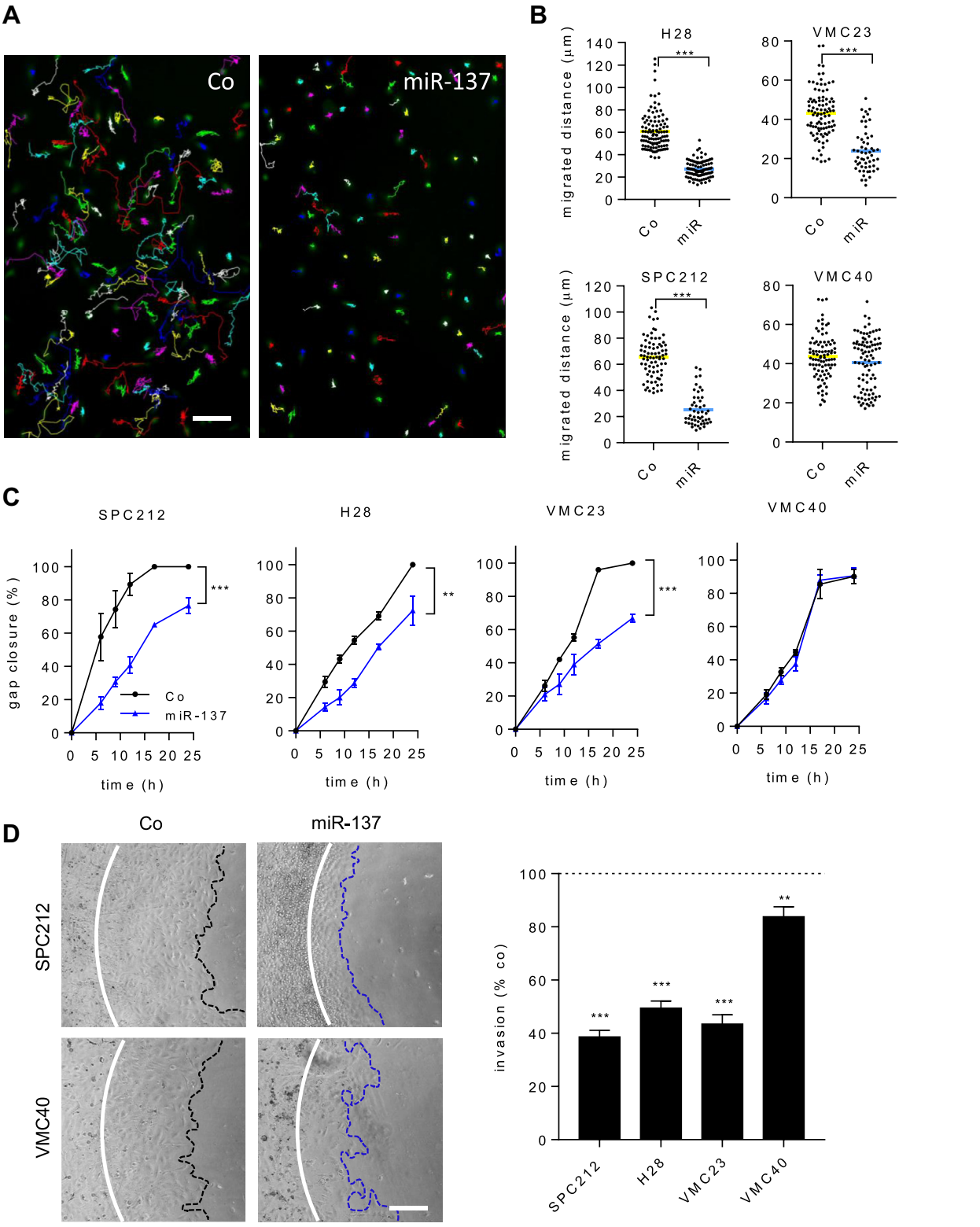

Figure 4. miR-137 inhibits malignant pleural mesothelioma (MPM) cell migration and invasion. (*A*) Representative pictures of manually tracked migration of H28 cells transfected with miR-137 or control (Co) mimics (5 nM) over 25 hours using ImageJ software. Scale bar = 100 μm. (B) Cumulative migrated distance (μm) of single cells transfected with miR-137 or Co mimics (5 nM) in 25 hours assessed by videomicroscopy. (*C*) Percentage gap closure of miR-137–transfected cells (5 nM) normalized to Cos after 12 hours in a wound healing assay. (*D*) Invasion of cells transfected with 5 nM miR-137 relative to respective Cos in an agar-spot (*white line*) invasion assay after 48 hours. Dotted lines represent invasion by Co- (*black*) and miR-137–transfected (blue) cells. Scale bar = 250 μm. $^{**}p < 0.01$, $^{***}p < 0.001$.

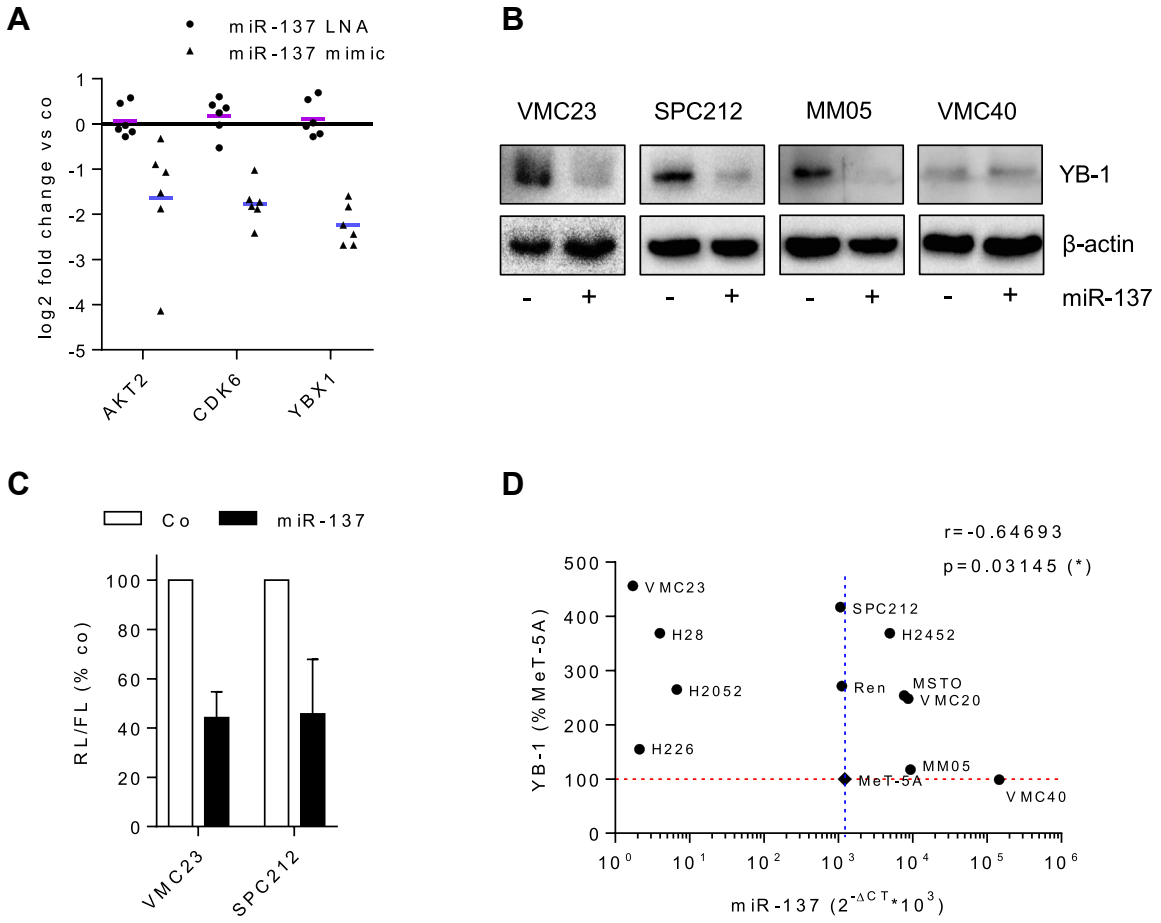

Figure 5. miR-137 suppresses oncoprotein YBX1, which is overexpressed in malignant pleural mesothelioma (MPM), by direct interaction with its mRNA. (*A*) Expression of three miR-137 target genes 48 hours after transfection with 5 nM miR-137 normaliZed to control (Co) mimics and 20 nM miR-137 locked nucleic acid inhibitor normalized to both negative inhibitor Cos in six MPM cell lines, determined by reverse-transcriptase quantitative polymerase chain reaction. 18S was used as a reference gene. (*B*) Immunoblot of YBX1 and β-actin (which served as loading Co) 72 hours after transfection with 5 nM of miR-137 (+) or Co (-) mimics. (*C*) Normalized percentage of luciferase activity (renilla-to-firefly ratio [RL/FL]) 48 hours after transfection with microRNA or Co mimics (5 nM) in two MPM cells. (*D*) Results of densitometry analysis of immunoblots after normalization to β-actin (*y* axis) and miR-137 expression levels (from reverse-transcriptase quantitative polymerase chain reaction [*x* axis]). Dotted lines indicate the levels of YBX1 and miR-137 in MeT-5A cells. A Spearman's rank correlation showed that there was a significant negative correlation ($r = -0.64693$, $p = 0.03145$).

assays showed that VMC40 (with low YBX1 levels) was only moderately affected, whereas VMC23 and SPC212 (high YBX1 levels) showed a significant decrease in cell growth by YBX1 reduction by siRNA alone and in combination with mimic (Fig. 6*A*). H28 cells were unaffected by YBX1 knockdown alone but showed significantly reduced growth in combination with miR-137, indicating that targets other than YBX1 are important to growth in this cell line. We also conducted colony formation, invasion, and motility assays. Importantly, YBX1 knockdown resulted in significantly impaired colony formation with miR-137 mimic or a combination of miR-137 and YBX1-siRNA (Fig. 6*B–D* and Supplementary Fig. 6), confirming that YB1 plays a substantial role in the miR-137–mediated regulation of the invasive behaviour of MPM cells.

Discussion

Recent reports have highlighted the important biological consequences of dysregulated miRNAs in MPM.[14,18,26–28] We have shown that miR-137 belongs to this list of aberrantly expressed miRNAs and that its target, YBX1, is important in the malignant characteristics of MPM. The considerable variation of miR-137 expression in cell lines and tumor samples suggests that it plays a complex role in MPM biology. LOH in the chromosomal region 1p21-22 (which includes *MIR137HG*) has been observed in MPM, although its consequence is largely unreported.[12] Abnormalities of 1p21-22 are linked to reduced patient survival in other tumor types, including multiple myeloma and plasma cell leukemia.[29,30] In the present study, we have shown that CNV of *MIR137HG* correlated with mature

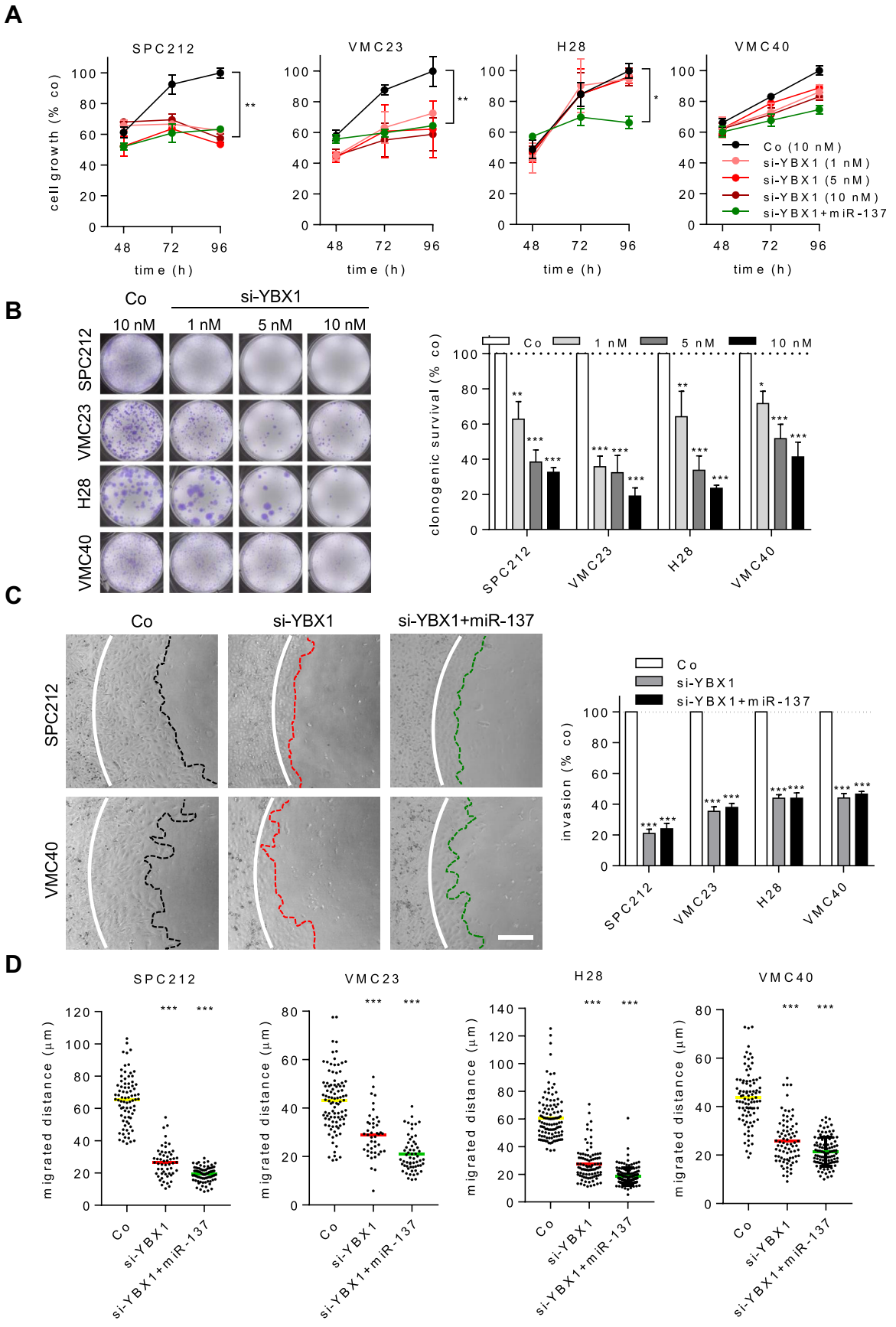
A
SPC212
VMC23
H28
VMC40
cell growth (% co)
time (h)
Co (10 nM)
si-YBX1 (1 nM)
si-YBX1 (5 nM)
si-YBX1 (10 nM)
si-YBX1+miR-137
B
Co
si-YBX1
10 nM
1 nM
5 nM
10 nM
clonogenic survival (% co)
C
Co
si-YBX1
si-YBX1+miR-137
invasion (% co)
D
migrated distance (µm)

microRNA expression in cell lines. In contrast, it was not related to expression in our cohort of F/F patient samples, although it should be noted that this series is small (n = 12). Taking this into account, we cannot rule out a role for CNV in the dysregulation of miR-137 in MPM, and further inquiry with a larger series of patient samples must be conducted to validate our findings.

As CNV alone did not conclusively explain the variable expression we observed, we investigated the role of promoter methylation in miR-137 variance in cell lines and patient samples. We have shown that 5-Aza treatment results in reexpression of miR-137 and have quantitatively demonstrated promoter methylation of *MIR137HG* (particularly in MPM cells with low basal expression), which is consistent with studies in other tumor types.[20] This supports the notion that methylation is a frequent cause of miR-137 silencing in MPM and suggests that a combination of CNV and promoter methylation leads to the dysregulation of miR-137. Contrary to our findings, studies of miR-137 expression in other tumor types report either a consistent upregulation or, more commonly, downregulation of miR-137.[19,20,31] Our data show that miR-137 expression in MPM can be split into three groups: high expressers, moderate expressers, and low expressers. Additionally, although high miR-137 expression is commonly associated with favorable prognosis in other cancers,[20,32] here we have shown that elevated miR-137 was associated with shorter survival in both series of patients with MPM. We did not see an effect of inhibiting miR-137 on target expression or cell growth but, somewhat unexpectedly, a miR-137 mimic demonstrated tumor suppressive activity in MPM cells, as evidenced by its ability to suppress proliferation, colony formation, migration, and invasion. Similar tumor suppressor effects of miR-137 have been observed in other cancers,[19,20,32] with the exception of bladder cancer, in which miR-137 acts as an oncogenic miRNA.[31]

Interestingly, although miR-137 loss has been implicated in early colorectal carcinogenesis,[19] another study found that elevated miR-137 was linked to shorter survival in patients with CRC.[33] This group also found that elevating miR-137 induced growth inhibition of CRC cell lines,[33] mirroring our results in MPM cells. It is possible that, similarly to what occurs in CRC, miR-137 loss is linked to MPM tumorigenesis and it plays a tumor suppressor role in early MPM. Then, as the tumor progresses and the biology of the cells change, elevated miR-137 results in increased aggressiveness, explaining its association with poor MPM prognosis. A similar counterintuitive relationship also exists for BAP1, a frequently mutated tumor suppressor in MPM. Germline 3p21 loss is associated with BAP1 cancer syndrome—an increased risk for development of certain cancer types such as mesothelioma.[8] Fascinatingly, although these individuals are more susceptible to MPM development, BAP1 loss significantly increases the median survival of patients with both familial and sporadic MPM after diagnosis.[34]

In this study, transfection of miR-137 mimic downregulated *CDK6*, *AKT-2,* and *YBX1* mRNA levels, and miR-137 directly inhibited the expression of YBX1 expression. MiR-137–mediated CDK6 suppression is linked to growth inhibition and G0/G1 cell cycle arrest,[20] whereas targeting AKT-2 in gastric cancer is linked to dampened tumorigenesis.[35] Other potentially interesting targets of miR-137 include cyclooxygenase 2,[36] which is known to be overexpressed in MPM,[37] and myeloid cell leukemia 1,[38] which we have shown to be oncogenic in MPM.[27] There was a significant negative correlation between YBX1 protein and miR-137 expression, implying a biologically relevant role for this interaction in MPM. When transfected with a combination of miR-137 mimic and *YBX1*-specific siRNA, most cells responded with reduced growth, whereas all demonstrated significant migration and invasion inhibition to a level similar as with mimic alone. This strongly implies that YBX1 is the most important miR-137 target contributing to migration and invasion in these cells.

YBX1 is an important factor in cancer cell growth, and its overexpression in tumors correlates with poor patient survival.[39] Studies have shown that miR-137–mediated YBX1 downregulation leads to reduced tumorigenic properties of other cancers.[40,41] YBX1 and its positive regulator twist family bHLH transcription factor 1 are expressed highly in sarcomatoid MPM, and both are linked to epithelial-mesenchymal transition.[42] Here, YBX1 was required for the proliferation of some

Figure 6. Y-box binding protein 1 gene (*YBX1*) knockdown inhibits malignant pleural mesothelioma (MPM) cell proliferation, colony formation, invasion, and migration. (*A*) Growth inhibition assay of MPM cell lines over 96 hours after transfection of YBX1 siRNA, miR-137 mimic or control (Co) small interfering (siRNA) (Co) at the indicated concentrations. Data are normalized to Co-transfected cells at 96 hours and expressed as mean plus or minus SE of the mean of the percentage of Co-transfected cells at 96 hours and representative of three independent experiments performed in triplicate. (*B*) Representative pictures and quantification of colonies formed in response to *YBX1*-specific or Co siRNA transfection at the indicated concentrations normalized to Co mimic stained with crystal violet. (*C*) Invasion of cells transfected with 5 nM *YBX1*-specific siRNA or in combination with 5 nM miR-137 mimic in relation to respective Cos in an agar-spot (*white line*) invasion assay after 48 hour. Scale bar = 250 μm. (*D*) Cumulative migrated distance (μm) of single cells transfected with miR-137 mimic or *YBX1*-specific or Co siRNAs (5 nM) in 25 hours assessed by videomicroscopy. $^{*}p < 0.05$, $^{**}p < 0.01$, $^{***}p < 0.001$.

cell lines and was essential in the colony-forming ability, migration, and invasion of all MPM cells tested, which is consistent with its role in the invasion and migration of other cancer cell types.[39] Taken together, our results show that YBX1 is an important target of miR-137, particularly as it is so integrally involved in invasion and migration of MPM, a malignancy characterized by aggressive local invasion. In addition to miR-137, other factors may contribute to the regulation of YB1 in MPM. Besides miR-137, several miRNAs are known to bind and down-regulate *YBX1*, such as miR-382.[43] In addition to miRNAs, twist family bHLH transcription factor 1 directly targets and enhances YB1 expression and is differentially expressed in sarcomatoid versus non-sarcomatoid MPM.[42,44]

The application of effective miRNA- and siRNA-based therapies is becoming feasible thanks to the development of novel miRNA delivery methods, such as EnGeneIC Dream Vector nanocells (EDVs).[45] We have performed several preclinical studies utilizing EDVs in MPM[26,27] and have completed a phase I clinical trial with intravenously administered miRNA-loaded EDVs.[18] Our functional data suggest that YB1 knockdown may have therapeutic significance. Interestingly, nude mice inoculated with NSCLC A549 cells transfected with *YBX1* siRNA showed impaired tumor growth compared with siRNA control–transfected cells.[46] Additionally, the ability of EDVs to deliver siRNAs[47] as well as miRNA mimics makes a strong case for use of *YBX1*-specific siRNAs in future in vivo MPM studies. Additional methods of YBX1 inhibition include use of a cell-permeable peptide able to inhibit YBX1 Serine 102 phosphorylation through molecular docking, which reduced YBX1–mediated growth inhibition and resistance to trastuzumab.[48] This may also be applicable in MPM and warrants further investigation.

In conclusion, our results indicate that miR-137 is dysregulated in MPM because of CNV and hypermethylation of the *MIR137HG* promoter. Furthermore, elevating miR-137 levels in cells inhibits the malignant characteristics of MPM. This activity is explained, at least in part, by targeting YBX1—an important factor in the colony formation, migration, and invasion of MPM cells. By characterizing an important biological interaction between two regulatory factors involved in the inherent invasiveness of MPM, our study furthers the understanding of MPM biology and provides potential targets for therapeutic intervention.

Acknowledgements

Dr. Johnson reports grants from Cancer Institute New South Wales (NSW) and grants from The Asbestos Diseases Foundation of Australia during the conduct of the study. Dr. Schelch reports grants from Cancer Institute NSW during the conduct of the study. Dr. Cheng reports grants from Cancer Institute NSW during the conduct of the study. Dr. Williams reports grants from Sydney Catalyst during the conduct of the study. Dr. Sarun reports grants from Cancer Institute NSW during the conduct of the study. Dr. Kirschner reports grants from Cancer Institute NSW and grants from Cancer Australia during the conduct of the study. Dr. Reid reports grants from Cancer Institute New South Wales and grants from Cancer Australia during the conduct of the study. This work was supported by a Cancer Institute NSW Translational Program Grant (11/TPG/3-06) to Drs. van Zandwijk and Reid; a Cancer Institute NSW Research Equipment Grant (15/REG/1-16) to Drs. van Zandwijk, Reid, and Dr. Lin; and a Cancer Australia Grant (1031821) to Dr Reid. Funding bodies were not involved in study design, collection, analysis, or interpretation of data; writing; or the decision to submit to the *Journal of Thoracic Oncology*. We thank M. A. Hoda, T. Klikovits, W. Klepetko, M. Eisenbauer, and A. Wagner for providing the VMC and Meso cell lines; R. Stahel for the SPC lines; K. Grankvist for P31; A. Catania for I2; V. L. Kinnula for M38K; and The Thoracic Research Centre (The Prince Charles Hospital, Brisbane, Australia) for MM05.

Supplementary Data

Note: To access the supplementary material accompanying this article, visit the online version of the *Journal of Thoracic Oncology* at www.jto.org and at https://doi.org/10.1016/j.jtho.2017.10.016.

References

1. Vogelzang NJ, Rusthoven JJ, Symanowski J, et al. Phase III study of pemetrexed in combination with cisplatin versus cisplatin alone in patients with malignant pleural mesothelioma. *J Clin Oncol*. 2003;21:2636–2644.
2. van Zandwijk N, Clarke C, Henderson D, et al. Guidelines for the diagnosis and treatment of malignant pleural mesothelioma. *J Thorac Dis*. 2013;5:E254–E307.
3. Linton A, Vardy J, Clarke S, et al. The ticking time-bomb of asbestos: its insidious role in the development of malignant mesothelioma. *Crit Rev Oncol/Hematol*. 2012;84:200–212.
4. Takahashi K, Landrigan PJ, Ramazzini C. The global health dimensions of asbestos and asbestos-related diseases. *Ann Glob Health*. 2016;82:209–213.
5. Bueno R, De Rienzo A, Dong L, et al. Second generation sequencing of the mesothelioma tumor genome. *PLoS One*. 2010;5:e10612.
6. Cheng JQ, Jhanwar SC, Klein WM, et al. p16 alterations and deletion mapping of 9p21–p22 in malignant mesothelioma. *Cancer Res*. 1994;54:5547–5551.
7. Chiosea S, Krasinskas A, Cagle PT, Mitchell KA, Zander DS, Dacic S. Diagnostic importance of 9p21 homozygous deletion in malignant mesotheliomas. *Mod Pathol*. 2008;21:742–747.

8. Carbone M, Yang H, Pass HI, Krausz T, Testa JR, Gaudino G. BAP1 and cancer. *Nat Rev Cancer*. 2013;13:153–159.
9. Chirac P, Maillet D, Leprêtre F, et al. Genomic copy number alterations in 33 malignant peritoneal mesothelioma analyzed by comparative genomic hybridization array. *Hum Pathol*. 2016;55:72–82.
10. Petrilli AM, Fernández-Valle C. Role of merlin/NF2 inactivation in tumor biology. *Oncogene*. 2016;35:537–548.
11. Yoshitaka S. Inactivation of merlin in malignant mesothelioma cells and the Hippo signaling cascade dysregulation. *Pathol Int*. 2011;61:331–344.
12. Murthy SS, Testa JR. Asbestos, chromosomal deletions, and tumor suppressor gene alterations in human malignant mesothelioma. *J Cell Physiol*. 1999;180:150–157.
13. Melaiu O, Bracci E, Cristaudo A, et al. Comparative genomic hybridization studies on mesothelioma show a parallel fate of 1p21-1p22 and 9p21 bands and a chromosomally stable sub-group. *Am J Med Biol Res*. 2013;1:149–158.
14. Ivanov SV, Goparaju CMV, Lopez P, et al. Pro-tumorigenic effects of miR-31 loss in mesothelioma. *J Biol Chem*. 2010;285:22809–22817.
15. Jonas S, Izaurralde E. Towards a molecular understanding of microRNA-mediated gene silencing. *Nat Rev Genet*. 2015;16:421–433.
16. Williams M. Exploring mechanisms of microRNA downregulation in cancer. *MicroRNA*. 2016;5:1–15.
17. Shah MY, Alessandra F, Sood AK, Lopez-Berestein G, Calin GA. MicroRNA therapeutics in cancer—an emerging concept. *EBioMedicine*. 2016;12:34–42.
18. Reid G, Kao SC, Pavlakis N, et al. Clinical development of TargomiRs, a miRNA mimic-based treatment for patients with recurrent thoracic cancer. *Epigenomics*. 2016;8:1079–1085.
19. Francesc B, Link A, Lozano JJ, et al. Epigenetic silencing of miR-137 is an early event in colorectal carcinogenesis. *Cancer Res*. 2010;70:6609–6618.
20. Joachim S, Lim DA, Petritsch C, et al. miR-124 and miR-137 inhibit proliferation of glioblastoma multiforme cells and induce differentiation of brain tumor stem cells. *BMC Med*. 2008;6:14.
21. Kao SC, Lee K, Armstrong NJ, et al. Validation of tissue microarray technology in malignant pleural mesothelioma. *Pathology*. 2011;43:128–132.
22. Linton A, Cheng YY, Griggs K, et al. An RNAi-based screen reveals PLK1, CDK1 and NDC80 as potential therapeutic targets in malignant pleural mesothelioma. *British J Cancer*. 2014;110:510–519.
23. Long-Cheng Li, Dahiya Rajvir. MethPrimer: designing primers for methylation PCRs. *Bioinformatics*. 2002;18:1427–1431.
24. Schneider CA, Rasband WS, Eliceiri KW. NIH Image to ImageJ: 25 years of image analysis. *Nat Methods*. 2012;9:671–675.
25. Cheng NC, van Zandwijk N, Reid G. Cilengitide inhibits attachment and invasion of malignant pleural mesothelioma cells through antagonism of integrins $\alpha v\beta 3$ and $\alpha v\beta 5$. *PloS One*. 2014;9:e90374.
26. Reid G, Pel ME, Kirschner MB, et al. Restoring expression of miR-16: a novel approach to therapy for malignant pleural mesothelioma. *Ann Oncol*. 2013;24:3128–3135.
27. Williams M, Kirschner MB, Cheng YY, et al. miR-193a-3p is a potential tumor suppressor in malignant pleural mesothelioma. *Oncotarget*. 2015;6:23480.
28. Kubo T, Toyooka S, Tsukuda K, et al. Epigenetic silencing of microRNA-34b/c plays an important role in the pathogenesis of malignant pleural mesothelioma. *Clin Cancer Res*. 2011;17:4965–4974.
29. Chang H, Ning Y, Qi X, Xu W. Chromosome 1p21 deletion is a novel prognostic marker in patients with multiple myeloma. *Br J Haematol*. 2007;139:51–54.
30. Chang H, Qi X, Yeung J, Reece D, Xu W, Patterson B. Genetic aberrations including chromosome 1 abnormalities and clinical features of plasma cell leukemia. *Leukemia Res*. 2009;33:259–262.
31. Xiu Y, Liu Z, Xia S, et al. MicroRNA-137 upregulation increases bladder cancer cell proliferation and invasion by targeting PAQR3. *PLoS One*. 2014;9:e109734.
32. Luo C, Tetteh PW, Merz PR, et al. miR-137 inhibits the invasion of melanoma cells through downregulation of multiple oncogenic target genes. *J Invest Dermatol*. 2013;133:768–775.
33. Sun Y, Xiaoping Z, Zhou Y, Hu Y. *Oncol Rep*. 2012;28:1346–1352.
34. Farzin M, Toon CW, Clarkson A, et al. Loss of expression of BAP1 predicts longer survival in mesothelioma. *Pathology*. 2015;47:302–307.
35. Wu L, Chen J, Ding C, et al. MicroRNA-137 contributes to dampened tumorigenesis in human gastric cancer by targeting AKT2. *PloS One*. 2015;10:e0130124.
36. Cheng Y, Li Y, Liu D, Zhang R, Zhang J. miR-137 effects on gastric carcinogenesis are mediated by targeting Cox-2-activated PI3K/AKT signaling pathway. *FEBS Lett*. 2014;588:3274–3281.
37. Marrogi A, Pass HI, Khan M, Metheny-Barlow LJ, Harris CC, Gerwin BI. Human mesothelioma samples overexpress both cyclooxygenase-2 (COX-2) and inducible nitric oxide synthase (NOS2): in vitro anti-proliferative effects of a COX-2 inhibitor. *Cancer Res*. 2000;60:3696–3700.
38. Yang Y, Li F, Saha MN, Abdi J, Qiu L, Chang H. miR-137 and miR-197 induce apoptosis and suppress tumorigenicity by targeting MCL-1 in multiple myeloma. *Clin Cancer Res*. 2015;21:2399–2411.
39. Lasham A, Woolley AG, Dunn SE, Braithwaite AW. YB-1: oncoprotein, prognostic marker and therapeutic target? *Biochem J*. 2013;449:11–23.
40. Guo Y, Pang Y, Gao X, et al. MicroRNA-137 chemosensitizes colon cancer cells to the chemotherapeutic drug oxaliplatin (OXA) by targeting YBX1. *Cancer Biomark*. 2016:1–9.
41. Zhu X, Li Y, Shen H, et al. miR-137 restoration sensitizes multidrug-resistant MCF-7/ADM cells to anticancer agents by targeting YB-1. *Acta Biochim Biophys Sin (Shanghai)*. 2013;45:80–86.

42. Iwanami T, Uramoto H, Nakagawa M, et al. Clinical significance of epithelial-mesenchymal transition-associated markers in malignant pleural mesothelioma. *Oncology*. 2014;86:109–116.
43. Xu M, Jin H, Xu CX, et al. miR-382 inhibits osteosarcoma metastasis and relapse by targeting Y box-binding protein 1. *Mol Ther*. 2015;23:89–98.
44. Shiota M, Yokomizo A, Itsumi M, et al. Twist1 and Y-box-binding protein-1 promote malignant potential in bladder cancer cells. *BJU Int*. 2011;108: E142–E149.
45. MacDiarmid JA, Mugridge NB, Weiss JC, et al. Bacterially derived 400 nm particles for encapsulation and cancer cell targeting of chemotherapeutics. *Cancer Cell*. 2007;11:431–445.
46. Lasham A, Samuel W, Cao H, et al. YB-1, the E2F pathway, and regulation of tumor cell growth. *J Natl Cancer Inst*. 2012;104:133–146.
47. MacDiarmid JA, Amaro-Mugridge NB, Madrid-Weiss J, et al. Sequential treatment of drug-resistant tumors with targeted minicells containing siRNA or a cytotoxic drug. *Nat Biotech*. 2009;27:643–651.
48. Law JH, Li Y, To K, et al. Molecular decoy to the Y-box binding protein-1 suppresses the growth of breast and prostate cancer cells whilst sparing normal cell viability. *PLoS One*. 2010;5:e12661.